Lateralized Reverse Shoulder Arthroplasty Maintains Rotational Function of the Remaining Rotator Cuff

Stefan Greiner, Christan Schmidt, Christian König, Carsten Perka & Sebastian Herrmann

Clinical Orthopaedics and Related Research®

ISSN 0009-921X

Clin Orthop Relat Res
DOI 10.1007/s11999-012-2692-x

Springer

Clin Orthop Relat Res
DOI 10.1007/s11999-012-2692-x

Clinical Orthopaedics and Related Research®
A Publication of The Association of Bone and Joint Surgeons®

BASIC RESEARCH

Lateralized Reverse Shoulder Arthroplasty Maintains Rotational Function of the Remaining Rotator Cuff

Stefan Greiner MD, Christan Schmidt, Christian König Dr Ing, Carsten Perka MD, Sebastian Herrmann MD

Received: 29 March 2012 / Accepted: 26 October 2012

Abstract

Background Humeral rotation often remains compromised after nonlateralized reverse shoulder arthroplasty (RSA). Reduced rotational moment arms and muscle slackening have been identified as possible reasons for this impairment. Although several clinical studies suggest lateralized RSA may increase rotation, it is unclear whether this is attributable to preservation of rotational moment arms and muscle pretension of the remaining rotator cuff.

Questions/purposes The lateralized RSA was analyzed to determine whether (1) the rotational moment arms and (2) the origin-to-insertion distances of the teres minor and subscapularis can be preserved, and (3) their flexion and abduction moment arms are decreased.

Methods Lateralized RSA using an 8-mm resin block under the glenosphere was performed on seven cadaveric shoulder specimens. Preimplantation and postimplantation CT scans were obtained to create three-dimensional shoulder surface models. Using these models, function-specific moment arms and origin-to-insertion distances of three segments of the subscapularis and teres minor muscles were calculated.

Results The rotational moment arms remained unchanged for the middle and caudal subscapularis and teres minor segments in all tested positions (subscapularis, −16.1 mm versus −15.8 mm; teres minor, 15.9 mm versus 15.3 mm). The origin-to-insertion distances increased or remained unchanged in any muscle segment apart from the distal subscapularis segment at 0° abduction (139 mm versus 145 mm). The subscapularis and teres minor had increased flexion moment arms in abduction angles smaller than 60° (subscapularis, 2.7 mm versus 8.3 mm; teres minor, −6.6 mm versus 0.8 mm). Abduction moment arms decreased for all segments (subscapularis, 4 mm versus −11 mm; teres minor, −3.6 mm versus −19 mm).

Conclusions After lateralized RSA, the subscapularis and teres minor maintained their length and rotational moment arms, their flexion forces were increased, and abduction capability decreased.

Clinical Relevance Our findings could explain clinically improved rotation in lateralized RSA in comparison to nonlateralized RSA.

The institution of one or more of the authors (SG, CS, CP, SH) received funding from the Robert-Mathys Research Foundation. All ICMJE Conflict of Interest Forms for authors and *Clinical Orthopaedics and Related Research* editors and board members are on file with the publication and can be viewed on request. *Clinical Orthopaedics and Related Research* neither advocates nor endorses the use of any treatment, drug, or device. Readers are encouraged to always seek additional information, including FDA-approval status, of any drug or device prior to clinical use. Each author certifies that his or her institution approved or waived approval for the reporting of this case and that all investigations were conducted in conformity with ethical principles of research. Each author confirms that he has read and agrees with the contents of this revised manuscript.

Electronic supplementary material The online version of this article (doi:10.1007/s11999-012-2692-x) contains supplementary material, which is available to authorized users.

S. Greiner (✉), C. Schmidt, C. Perka, S. Herrmann
Center for Musculoskeletal Surgery, Charité-University Medicine Berlin, Charitéplatz 1, D-10117 Berlin, Germany
e-mail: stefan.greiner@charite.de

C. König
Julius Wolff Institute, Charité University Medicine Berlin, Berlin, Germany

Introduction

Early reverse shoulder arthroplasties (RSAs) of the 1970s had rates of implant failure ranging from 15% to 35%

Published online: 01 December 2012

[8, 19, 23]. The essential structural changes made in the construction of the reverse shoulder prosthesis as introduced by Grammont and Baulot are (1) medialization of the center of rotation; (2) use of a larger ball on the glenoid component; (3) implementation of 155° nonanatomic humeral inclination; and (4) distalization of the deltoid insertion [14]. These changes result in an increased deltoid lever arm and reduced torque on the glenoid component owing to the position of the center of rotation at the prosthesis-bone interface [5]. Improved shoulder function and pain reduction at 2 to 5 years has been observed with the "Grammont-type" design [4, 9, 15, 29], and survival at 10 years free of revision is reportedly 89% [10]. However, a decrease in patient function apparently occurs at 6 to 8 years followup [10, 26] and the rate of patients having a Constant-Murley score less than 30 is reportedly 72% at 10 years [10]. Although most patients show a major gain in active flexion and abduction [4, 6, 7, 10, 22, 25, 29], active external and internal rotation often remains unchanged and can be reduced after the procedure [5, 15, 29]. Loss of active rotation of the shoulder limits the activities of daily living such as combing hair, dressing, bringing a full glass to the mouth, performing personal hygiene tasks, and controlling the spatial position of the arm [1, 2, 25].

Function of the remaining rotator cuff is important for shoulder rotation and patient function. Although the teres minor and/or subscapularis muscle-tendon unit may be intact in patients with cuff tear arthropathy [1, 2, 25], rotational capability after nonlateralized RSA remains limited regardless of the postoperative integrity of the teres minor and/or subscapularis muscle [7, 25]. Medialization of the rotational center may explain these findings, because it leads to major changes in the muscle pretensioning and rotational moment arms of the remaining rotator cuff [5]. We previously studied the changes in moment arms and origin-to-insertion distances of the teres minor and subscapularis in a three-dimensional (3-D) cadaveric CT scan model before and after nonlateralized RSA. We found decreases in rotational moment arms as much as 36% for the cranial segments of the subscapularis and 25% in all segments of the teres minor after implantation of the prosthesis. Moreover, the origin-to-insertion distance values were reduced by 7 mm to 20 mm at 15° and 30° abduction [17]. These biomechanical disadvantages could be offset through lateralization of the center of rotation in RSA. One possible technique for lateralization of the center of rotation is the bony increased offset RSA technique with an autologous bone interposed between the glenoid and the glenosphere [3]. Moreover, specific implants with an increased offset intrinsic to the glenoid component could be used to achieve lateralization [9]. The degree of lateralization often can be varied depending on the glenosphere used with a maximum of as much as 10 mm. With both techniques, active rotation appears superior to that without lateralization [3, 21]. However, whether rotational moment arms and muscle pretension of the remaining rotator cuff are preserved with a lateralized RSA and therefore may help to improve rotation has not been evaluated so far.

Lateralized RSA was analyzed to determine whether (1) the rotational moment arms and (2) the origin-to-insertion distances of the teres minor and subscapularis can be preserved, and (3) their flexion and abduction moment arms are decreased.

Materials and Methods

We tested seven fresh-frozen human shoulder specimens (mean age, 74 years; range, 61–82 years). Specimens having a history or showing signs of previous surgery, trauma, deformities, or severe osteoarthritis were not used. We used six right shoulders and one left shoulder. To evaluate possible changes in moment arms and origin-to-insertion distances, 3-D surface models were created from CT scans before and after lateralized RSA was performed. A mathematic script calculated function-specific moment arms for humeral rotation, flexion and extension, and abduction and adduction based on muscle-specific landmarks in the 3-D models.

In a previous study, rotational moment arms of the subscapularis and teres minor were calculated using the same method as in the current study on seven shoulder specimens [17]. Using this method, the rotational moment arms for the subscapularis and teres minor had a mean of 16 mm in native shoulders with a maximum SD of 2.8 mm. Based on the data obtained in this study, a power analysis was performed using SPSS SamplePower 3.0 (IBM, Armonk, NY, USA). Assuming an α error of 0.05 and a power of 0.80, it was anticipated that seven specimens would be required in each group to show a 4-mm difference, which represents a 25% change of the mean rotational moment arms. Alpha level correction was not considered in the sample size calculation.

The specimens were further prepared using a previously described protocol [17]. We identified bony landmarks necessary for analysis and marked them using radiopaque pins. Predefined marking of the bony landmarks included the center of the medial and lateral epicondyles of the elbow. We marked the teres minor using two pins at its insertion to the greater tuberosity and at its origin in the region of the lateral posterior rim of the scapula. We marked the subscapularis insertion area at the lesser tuberosity with two pins at its laminar origin at the scapula. Additional markers were inserted on the scapula side at the acromial, medial, and inferior angles. After preparation, we implanted a polycarbonate resin model of a reverse

shoulder prosthesis (Mathys AG, Bettlach, Switzerland) in a standardized manner. This implant is equivalent to the company's reverse shoulder prosthesis model (Affinis Inverse®). The glenoid component had a diameter of 39 mm with no additional offset. The glenoid surface was reamed until punctual perforation of the subchondral bone was evident. Lateralization was achieved using an 8 × 39-mm resin block that was implanted between the baseplate of the glenosphere and the glenoid (Fig. 1). The block with the glenosphere was implanted to fit exactly at the inferior border of the glenoid. The humeral component consisted of a size 6 stem with a length of 110 mm and inclination angle of 155°. We set the humeral retroversion angle, as measured by the forearm axis, to 10° in all specimens.

We scanned specimens before and after implantation using a 64-detector row scanner with a slice thickness of 0.5 mm and a resolution of 512 × 512 pixels (Aquilion 64; Toshiba Medical Systems, Otawara, Japan). All CT examinations were performed at 120 kV and a maximum tube current of 400 mA. Using 3-D data visualization, analysis, and modeling software (AMIRA Version 5.2.0; Visage Imaging, Inc, San Diego, CA, USA), we determined the spatial position of all previously marked landmarks and 3-D models of the humerus and the scapula were created for each specimen. With the landmarks and the 3-D surface models, joint coordinate systems were defined in the scapula and the humerus according to the recommendations of the International Society of Biomechanics (Fig. 1) [30]. According to these recommendations, the scapula coordinate system originates at the acromial angle and is defined by three bony, scapular landmarks. The coordinate system's x-axis points anteriorly (representing the abduction and adduction axis), the y-axis points cranially (representing the rotational axis), and the z-axis points laterally (representing the flexion and extension axis of the glenohumeral joint). The humeral coordinate system is defined by two bony landmarks—the medial and the lateral epicondyle and the center of the humeral head. The anatomic directions of the axes were equivalent to the coordinate system of the scapula. To determine the center of the humeral head, we fit a sphere into the computer model at the humeral articular surface using a least square fit algorithm [24]. Because these recommendations are applicable only for right shoulders, the one left shoulder used a mirrored protocol.

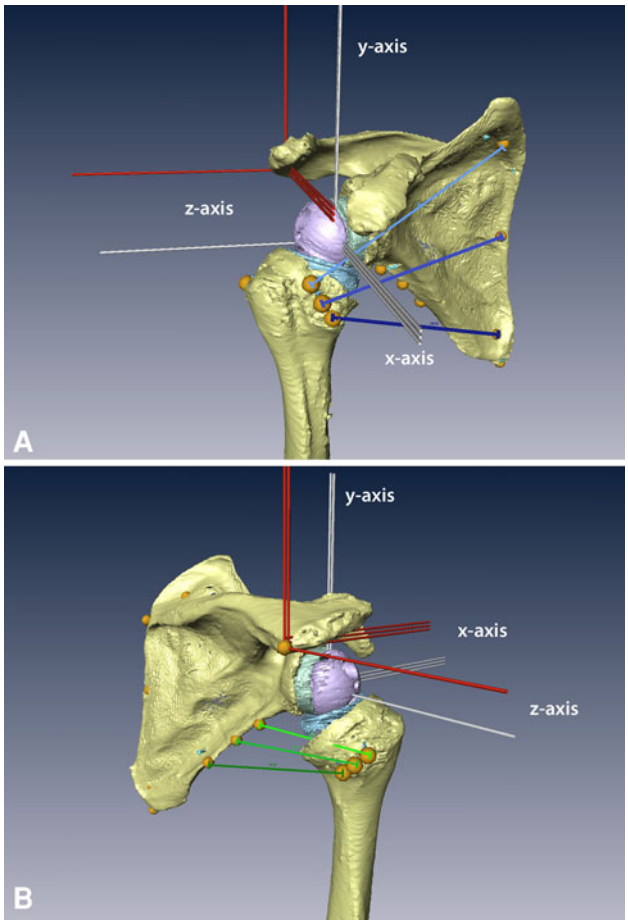

Fig. 1A–B (**A**) Anterolateral and (**B**) posterolateral views of the humerus and scapula in the 3-D model are shown. The glenosphere is lateralized by an 8-mm resin block (green). To align the humerus and scapula, two coordinate systems were defined (red lines, scapula coordinate system; white lines, humeral coordinate system). The subscapularis and teres minor are each represented by three lines (subscapularis, blue lines; teres minor, green lines).

We defined function-specific moment arms using the anatomic axes of glenohumeral motion ranges. A positive moment arm relative to the scapular z-axis is associated with humeral flexion motion. Conversely, negative values are associated with extension motions. A negative moment arm with respect to the y-axis is associated with the muscle's capability to internally rotate the humerus, whereas positive values are associated with external rotation. Finally, positive values with respect to the x-axis indicate abduction capability and negative values indicate adduction potential. Humeral position was expressed relative to the coordinate system of the scapula.

We calculated all moment arms and origin-to-insertion distances using the 3-D, virtual model derived from the CT scans. All analyses were performed according to a previously described protocol [17]. First, the 0° (neutral) position was defined with the humeral and scapular coordinate systems in line. We performed virtual humeral abduction of 30°, 45°, and 60° to analyze a representative range of glenohumeral motion in this plane.

For moment arm calculation, the teres minor and subscapularis were represented by three segments, which were modeled as lines between the muscles' origin and insertion points (Fig. 1). We did not consider wrapping these muscles. Moment arms for abduction and adduction, flexion

and extension, and external and internal rotation for three segments of each muscle were acquired using the origin-to-insertion method, as previously described [17, 18, 28].

To calculate individual rotational moment arms, we determined the total moment arm and then multiplied that by the unit vector belonging to that specific rotation:

$$M_{rot\_axis} = (\vec{r} \times \vec{F}) \cdot \vec{e}_{rot\_axis}$$

To obtain the moment arm for each rotation (l_{rot_axis}), the calculated moment then is divided by the absolute value of the acting force:

$$l_{rot\_axis} = \frac{(\vec{r} \times \vec{F})}{|\vec{F}|} \cdot \vec{e}_{rot\_axis}$$

$$l_{rot}^{hum} = (\vec{r}^{hum} \times \vec{u}^{hum}) \cdot \vec{e}_{y}^{hum} = r_{z}^{hum} u_{x}^{hum} - r_{x}^{hum} u_{z}^{hum}$$

Simplification of the formula allowed use of the unit vector of the acting force $\vec{u}$ instead of specific muscle forces. The moment arms therefore are dependent on the vector ($\vec{r}$) pointing from the center of rotation to the point of muscle force application and the direction of the force ($\vec{u}$).

We determined differences in rotational moment arms and origin-to-insertion distances between shoulders before and after implantation using the paired, two-sided t-test with Bonferroni correction for multiple comparisons. The same test was used to determine differences in flexion and extension and abduction and adduction moment arms. Normal distribution of tested parameters was confirmed using the Kolmogorov-Smirnov test. Statistical analysis was performed using SPSS Version 18 software (SPSS, Inc, Chicago, IL, USA), except the power analysis, which was performed using SPSS SamplePower 3.0 (IBM, Armonk, NY USA).

Results

The postimplantation calculated rotational moment arms of all subscapularis and teres minor segments were similar to their preimplantation values regardless of adjusted position (Fig. 2).

Origin-to-insertion distances of both muscles remained unchanged or increased postimplantation in any tested position apart from the distal subscapularis segment at 0° abduction. In this position, the origin-to-insertion distance decreased from 160 mm preimplantation to 145 mm postimplantation ($p = 0.07$). At 30° abduction the cranial subscapularis segment showed increased origin-to-insertion distance values (119 mm versus 134 mm; $p = 0.5$), whereas the other distal subscapularis and all teres minor segments had no major changes postimplantation. At 45° and 60° abduction, all segments had increased origin-to-insertion distance values. The maximum overall gain before versus after implantation occurred at 60° abduction. It was 17 mm for the subscapularis (cranial segment) and 13 mm for the teres minor (distal segment) (Fig. 3).

Calculated flexion moment arms of all subscapularis segments increased postimplantation in the 0°, 30°, and 45° positions. At 60°, only the cranial and middle segments had increased values, whereas the distal segments remained unchanged. Accordingly all segments of the teres minor

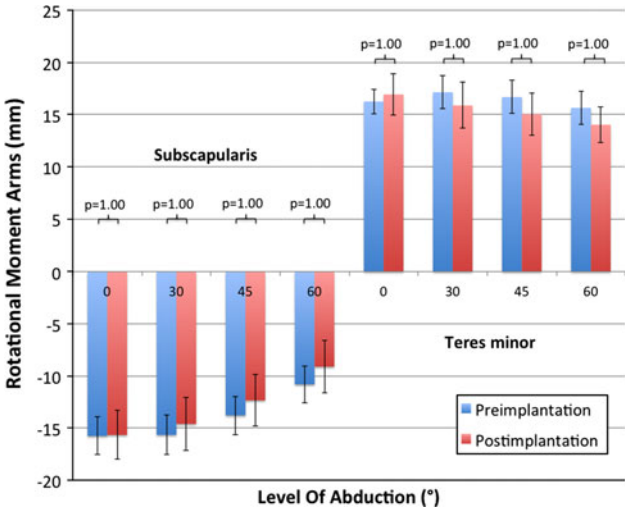

Fig. 2 Values for rotational moment arms (mm) of the subscapularis and teres minor (middle segments) before and after lateralized RSA are shown. Positive values express external rotation capability. No difference can be seen preimplantation versus postimplantation for this segment.

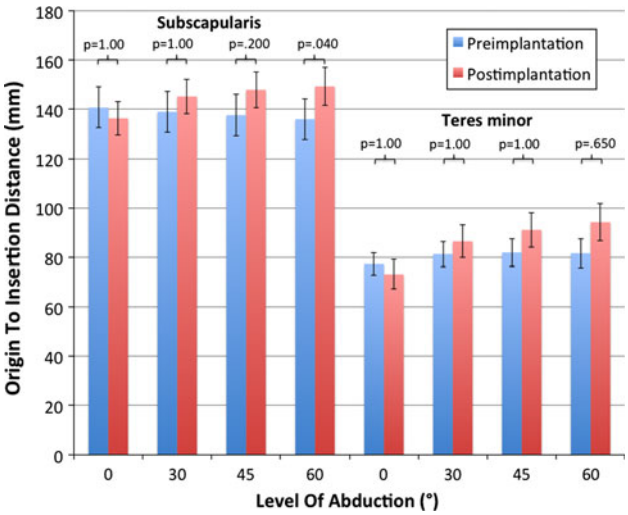

Fig. 3 Values for origin-to-insertion distances (mm) of the subscapularis and teres minor (middle segments) before and after lateralized RSA are shown. Postimplantation origin-to-insertion distance remained unchanged at 0° abduction. At 30° abduction and greater both muscles show increased origin-to-insertion distance values.

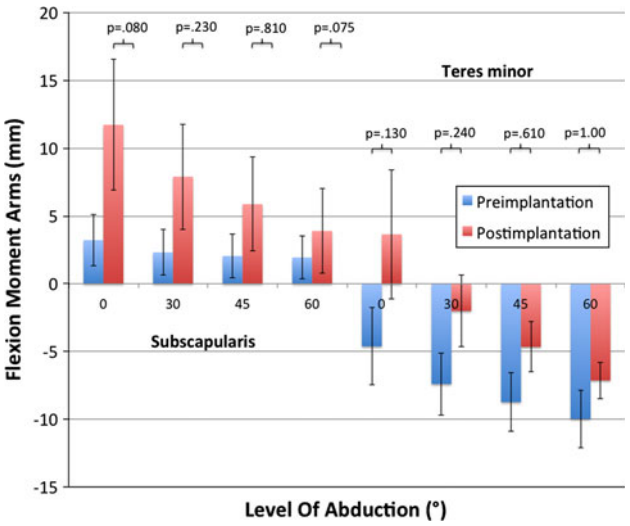

Fig. 4 Values for flexion moment arms (mm) of the subscapularis and teres minor (middle segments) before and after lateralized RSA are shown. Postimplantation flexion moment arms were increased at 0° to 45° abduction.

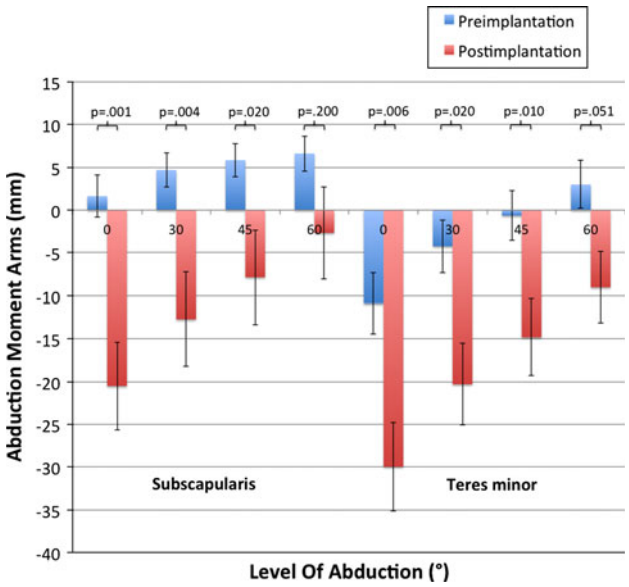

Fig. 5 Values for abduction and adduction moment arms (mm) of the subscapularis and teres minor (middle segments) before and after lateralized RSA are shown. Postimplantation abduction moment arms decreased in all positions, except for the 60° position compared with preimplantation values.

showed increased flexion moment arms apart from the distal segment at 60° abduction. This increase is most pronounced at 0° for the distal subscapularis and teres minor segments (before versus after implantation: subscapularis, 12.8 mm versus 22.7 mm, $p = 0.057$; teres minor, −2.9 mm versus 5.4 mm, $p = 0.44$) (Fig. 4). Both muscles had decreased abduction moment arms postimplantation except for the cranial subscapularis segment in 60° abduction. The cranial and middle subscapularis segments had positive values preoperatively, representing the abduction capability of these segments. Only the cranial segment had positive (abduction) moment arms at 45° and 60° postimplantation, whereas negative (adduction) moment arms were seen for all other segments. Therefore, there was loss of function of the subscapularis as an abductor in shoulder movement, whereas the adduction capability increased (Fig. 5) (Supplemental materials are available with the online version of CORR®).

Discussion

RSA for treatment of an irreparable rotator cuff tear in a patient with osteoarthritis generally improves flexion and abduction. In contrast, external and internal rotation remains compromised or even decreased after nonlateralized RSA [5, 25, 29]. Reduced rotational moment arms of the remaining rotator cuff in conjunction with decreased origin-to-insertion distances may be responsible for the functional impairment [17]. Recent clinical studies suggest lateralized RSA may improve active rotation in the presence of cuff tear arthropathy [3, 12, 27]. However, whether rotational moment arms and muscle pretension of the remaining rotator cuff are preserved in a lateralized RSA and therefore may help to improve rotation have not been evaluated so far. Therefore the lateralized RSA was analyzed to determine whether (1) the rotational moment arms and (2) the origin-to-insertion distances of the teres minor and subscapularis can be preserved, and (3) their flexion and abduction moment arms are decreased.

This study has some limitations. First, our specimens came from cadaveric specimens of individuals having no major deformity or cranialization of the humeral head as seen in patients with cuff tear arthropathy. Moment arms and origin-to-insertion distances may be different in specimens having rotator cuff arthropathy. However, the intraindividual approach comparing the moment arms and muscle length before and after implantation of the lateralized RSA reproducibly shows the changes resulting from the implant. Second, we used an in vitro and in silico approach based on 3-D models derived from CT scans. Although CT scans provide accurate data for modeling bony structures, muscle course and volume cannot be reproduced reliably. Therefore, muscles were represented using straight lines between the marked origin and insertion sites. Although data gathered using this method could differ owing to the simplicity of this model, the detected differences before and after inserting the implant are not likely to be affected substantially because muscle origin, insertion, and volume are not altered by the implant. Furthermore, preoperative moment arms calculated using the

presented method are comparable to data from previous studies using other methods [11, 13]. Third, we used a 39-mm glenoid component in all specimens. Diameters of glenospheres on the market range from 32 mm to 44 mm. The 39-mm implant was chosen to represent average sizing. Although changes in moment arms and origin-to-insertion distances may be different with differing component sizes, our data show the average changes using standard implants. Fourth, we had no control group evaluating the investigated parameters in nonlateralized RSA. However, using the same method, these findings were described previously [17], therefore allowing comparison to the current findings. Fifth, in powering the study we assumed a 25% change of the mean rotational moment arms would be clinically important although we are unaware of clinical data to support this assumption. However, our findings are consistent with the clinically observed improved rotation [3, 9, 27].

Our observations suggest lateralized RSA preserves rotational moment arms of the teres minor and the subscapularis (Fig. 2). In contrast, in a previous study [17] analyzing the effect of nonlateralized RSA on rotational moment arms, there were decreases in the cranial and middle segments of the subscapularis in all positions. Additionally, the rotational moment arm of the teres minor was decreased in all segments at greater than 15° abduction [17]. These findings could help explain improved rotational function after lateralized RSA. In a recent study using a lateralized glenoid component, Valenti et al. reported a gain of 15° to 30° external rotation [27]. Internal rotation was increased by 1 point according to the Constant-Murley score [27]. Boileau et al. also reported increased postimplantation external rotation using the bony increased offset RSA technique [3]. Using this method, an autologous bone is interposed between the glenoid and the glenosphere, thus achieving lateralization of the center of rotation. They observed no signs of glenoid loosening or graft resorption at a mean of 28 months [3]. Cuff et al. reported a major increase in patients treated with the increased offset Encore® Reverse Shoulder Prosthesis (DJO Surgical, Austin, TX, USA) [9]. Mulieri et al. reported an increase from 27° to 51° external rotation using the same implant in patients with irreparable rotator cuff tears without osteoarthritis [21]. However, these studies lacked control groups to confirm their findings compared with a nonlateralized RSA and lateralization carries the potential risk of higher implant-bone shear load using increased offset glenospheres or nonunion and graft resorption using bone grafting. Regardless, increased external rotation in lateralized RSA is obvious compared with nonlateralized clinical results. Our findings could explain this advantage of lateralized RSA, although other factors such as reduction of prosthetic impingement [16] and recruitment of posterior deltoid fibers [5] also may contribute.

Origin-to-insertion distances of the teres minor and subscapularis almost consistently remained unchanged or increased with abduction postimplantation (Fig. 3). For the subscapularis, this is in contrast to the preoperative situation. The insertion of the subscapularis at the lesser tuberosity is in the anatomic situation at approximately the level of the center of rotation. Therefore, there is no major change of its origin-to-insertion distance during abduction. For the teres minor, in the anatomic situation, there is a major increase of origin-to-insertion distance with higher degrees of abduction. The reason is the insertion of the teres minor, which is caudal to the center of rotation in the 0° position and becomes more lateral during abduction. Because RSA always leads to (further) distalization of the insertion of the subscapularis and teres minor in relation to the center of rotation, a change of the origin-to-insertion distance during abduction cannot be prevented. In contrast, previously published data regarding the change of origin-to-insertion distance after nonlateralized RSA showed a decrease for the teres minor in 30° or less abduction and for the middle and distal segments of the subscapularis at 15° abduction [17].

We found muscle tension was preserved with a lateralized RSA and the investigated amount of lengthening was not likely to hinder reconstruction nor lead to overtensioning of either of the muscles. Maintenance of muscle tension also might have a positive influence on rotational capability and capability to generate compressive forces.

The teres minor and subscapularis have abduction and adduction and flexion and extension capabilities in the native glenohumeral joint. Their balanced distribution in the AP (x) axis and their opposite positioning regarding the craniocaudal (y) axis results in the principle of concavity compression [20]. After a lateralized RSA, a major inferior shift of insertions of both muscles relative to the rotational center is seen. This results in loss of abduction and gain in flexion capabilities (Figs. 4, 5). However, comparison of the current data with previously published data using the same model for nonlateralized RSA [17] showed the decrease of abduction capability of both muscles is less in a lateralized RSA, whereas the gain in flexion capability remains comparable.

In contrast to a nonlateralized RSA, lateralization of the center of rotation is able to preserve rotational moment arms of the subscapularis and teres minor muscles and to maintain their muscle pretension. Changes in abduction and flexion capabilities of these muscles are reduced but cannot be completely avoided. These findings may partially explain the superior clinical results regarding rotational capability after lateralized RSA in comparison to nonlateralized RSA.

References

1. Boileau P, Chuinard C, Roussanne Y, Bicknell RT, Rochet N, Trojani C. Reverse shoulder arthroplasty combined with a modified latissimus dorsi and teres major tendon transfer for shoulder pseudoparalysis associated with dropping arm. *Clin Orthop Relat Res.* 2008;466:584–593.
2. Boileau P, Chuinard C, Roussanne Y, Neyton L, Trojani C. Modified latissimus dorsi and teres major transfer through a single delto-pectoral approach for external rotation deficit of the shoulder: as an isolated procedure or with a reverse arthroplasty. *J Shoulder Elbow Surg.* 2007;16:671–682.
3. Boileau P, Moineau G, Roussanne Y, O'Shea K. Bony Increased-offset reversed shoulder arthroplasty: minimizing scapular impingement while maximizing glenoid fixation. *Clin Orthop Relat Res.* 2011;469:2558–2567.
4. Boileau P, Watkinson D, Hatzidakis AM, Hovorka I. Neer Award 2005: The Grammont reverse shoulder prosthesis: results in cuff tear arthritis, fracture sequelae, and revision arthroplasty. *J Shoulder Elbow Surg.* 2006;15:527–540.
5. Boileau P, Watkinson DJ, Hatzidakis AM, Balg F. Grammont reverse prosthesis: design, rationale, and biomechanics. *J Shoulder Elbow Surg.* 2005;14(1 suppl):147S–161S.
6. Boulahia A, Edwards TB, Walch G, Baratta RV. Early results of a reverse design prosthesis in the treatment of arthritis of the shoulder in elderly patients with a large rotator cuff tear. *Orthopedics.* 2002;25:129–133.
7. Clark JC, Ritchie J, Song FS, Kissenberth MJ, Tolan SJ, Hart ND, Hawkins RJ. Complication rates, dislocation, pain, and postoperative range of motion after reverse shoulder arthroplasty in patients with and without repair of the subscapularis. *J Shoulder Elbow Surg.* 2012;21:36–41.
8. Coughlin MJ, Morris JM, West WF. The semiconstrained total shoulder arthroplasty. *J Bone Joint Surg Am.* 1979;61:574–581.
9. Cuff D, Pupello D, Virani N, Levy J, Frankle M. Reverse shoulder arthroplasty for the treatment of rotator cuff deficiency. *J Bone Joint Surg Am.* 2008;90:1244–1251.
10. Favard L, Levigne C, Nerot C, Gerber C, De Wilde L, Mole D. Reverse prostheses in arthropathies with cuff tear: are survivorship and function maintained over time? *Clin Orthop Relat Res.* 2011;469:2469–2475.
11. Favre P, Sheikh R, Fucentese SF, Jacob HA. An algorithm for estimation of shoulder muscle forces for clinical use. *Clin Biomech (Bristol, Avon).* 2005;20:822–833.
12. Frankle M, Siegal S, Pupello D, Saleem A, Mighell M, Vasey M. The reverse shoulder prosthesis for glenohumeral arthritis associated with severe rotator cuff deficiency: a minimum two-year follow-up study of sixty patients. *J Bone Joint Surg Am.* 2005;87:1697–1705.
13. Gatti CJ, Dickerson CR, Chadwick EK, Mell AG, Hughes RE. Comparison of model-predicted and measured moment arms for the rotator cuff muscles. *Clin Biomech (Bristol, Avon).* 2007;22:639–644.
14. Grammont PM, Baulot E. Delta shoulder prosthesis for rotator cuff rupture. *Orthopedics.* 1993;16:65–68.
15. Grassi FA, Murena L, Valli F, Alberio R. Six-year experience with the Delta III reverse shoulder prosthesis. *J Orthop Surg (Hong Kong).* 2009;17:151–156.
16. Gutierrez S, Comiskey CA 4th, Luo ZP, Pupello DR, Frankle MA. Range of impingement-free abduction and adduction deficit after reverse shoulder arthroplasty: hierarchy of surgical and implant-design-related factors. *J Bone Joint Surg Am.* 2008;90:2606–2615.
17. Herrmann S, Konig C, Heller M, Perka C, Greiner S. Reverse shoulder arthroplasty leads to significant biomechanical changes in the remaining rotator cuff. *J Orthop Surg Res.* 2011;6:42.
18. Hughes RE, Niebur G, Liu J, An KN. Comparison of two methods for computing abduction moment arms of the rotator cuff. *J Biomech.* 1998;31:157–160.
19. Lettin AW, Copeland SA, Scales JT. The Stanmore total shoulder replacement. *J Bone Joint Surg Br.* 1982;64:47–51.
20. Lippitt S, Matsen F. Mechanisms of glenohumeral joint stability. *Clin Orthop Relat Res.* 1993;291:20–28.
21. Mulieri P, Dunning P, Klein S, Pupello D, Frankle M. Reverse shoulder arthroplasty for the treatment of irreparable rotator cuff tear without glenohumeral arthritis. *J Bone Joint Surg Am.* 2010;92:2544–2556.
22. Nolan BM, Ankerson E, Wiater JM. Reverse total shoulder arthroplasty improves function in cuff tear arthropathy. *Clin Orthop Relat Res.* 2011;469:2476–2482.
23. Post M, Haskell SS, Jablon M. Total shoulder replacement with a constrained prosthesis. *J Bone Joint Surg Am.* 1980;62:327–335.
24. Schneider PJ, Eberly DH. Least Squares Fitting. *Geometric Tools for Computer Graphics*. San Francisco, CA: Morgan Kaufmann Publishers; 2003:882–889.
25. Simovitch RW, Helmy N, Zumstein MA, Gerber C. Impact of fatty infiltration of the teres minor muscle on the outcome of reverse total shoulder arthroplasty. *J Bone Joint Surg Am.* 2007;89:934–939.
26. Sirveaux F, Favard L, Oudet D, Huquet D, Walch G, Mole D. Grammont inverted total shoulder arthroplasty in the treatment of glenohumeral osteoarthritis with massive rupture of the cuff: results of a multicentre study of 80 shoulders. *J Bone Joint Surg Br.* 2004;86:388–395.
27. Valenti P, Sauzieres P, Katz D, Kalouche I, Kilinc AS. Do less medialized reverse shoulder prostheses increase motion and reduce notching? *Clin Orthop Relat Res.* 2011;469:2550–2557.
28. van der Helm FC. A finite element musculoskeletal model of the shoulder mechanism. *J Biomech.* 1994;27:551–569.
29. Werner CM, Steinmann PA, Gilbart M, Gerber C. Treatment of painful pseudoparesis due to irreparable rotator cuff dysfunction with the Delta III reverse-ball-and-socket total shoulder prosthesis. *J Bone Joint Surg Am.* 2005;87:1476–1486.
30. Wu G, van der Helm FC, Veeger HE, Makhsous M, Van Roy P, Anglin C, Nagels J, Karduna AR, McQuade K, Wang X, Werner FW, Buchholz B; International Society of Biomechanics. ISB recommendation on definitions of joint coordinate systems of various joints for the reporting of human joint motion: Part II. Shoulder, elbow, wrist and hand. *J Biomech.* 2005;38:981–992.